DOI: https://doi.org/10.54966/jreen.v27i1.1137 - *Journal of Renewable Energies 27 (2024) 15 – 33*

Journal of Renewable Energies

Revue des Energies Renouvelables

journal home page: https://revue.cder.dz/index.php/rer

Research paper

An efficient, intelligent PSO-P&O-PI MPPT mechanism for Photovoltaic Systems under variable climatic conditions

Layachi Zaghba *, Abdelhalim Borni ,Messaouda Khennane, Amor Fezzani and Abdelhak Bouchakour

Unité de Recherche Appliquée en Energies Renouvelables, URAER, Centre de Développement des Energies Renouvelables, CDER, 47133, Ghardaïa, Alegria.

ARTICLE INFO

Article history:
Received October 3, 2023
Accepted February 6, 2024

Keywords:
Fixed mount PV system,
Dual axis tracking,
MPPT,
PSO-P&O-PI,
Performance.

ABSTRACT

In recent years, there has been a global challenge in developing MPPT algorithms that provide maximum power efficiency. This paper deals with a novel P&O-PI MPPT mechanism where the soft computing technique called particle swarm optimization (PSO) is used to tune the PI parameters. The proposed approach was designed to improve the tracking response time of MPP with high efficiency. This MPPT is applied to two types of PV systems: tracking systems and fixed systems. The energy gain of a dual-axis tracker was compared to that of a fixed system. Simulation results were carried out in Matlab and Simulink environments to demonstrate the effectiveness of the suggested control strategy in terms of productivity, efficiency, and oscillations under different fast environmental conditions. We can see that the recommended technique shows excellent performance in terms of power overshoot, low oscillation, and response time. The PSO-P&O-PI-algorithm offers a considerable improvement in tracking efficiency of 99.90% and a time response of 0.023 s. We have demonstrated the significance of involving the sun-tracker PV system regarding produced power (acquired power) with around 25% energy gain, particularly during the less sunny hours.

1. INTRODUCTION

For the delivery of the greatest amount of power from the PV field, a variety of conventional MPPT algorithms have been investigated, including the short-circuit current method (Danandeh and Mousavi, 2018; Vijayakumari, 2021), the open-circuit voltage method (Huang and Hsu, 2016; Hassan et al. 2023), the perturb and observe (P&O) method (Alik and Jusoh, 2017; Kota and Bhukya, 2017), the incremental

* *Corresponding author, E-mail address: l.zaghba@cder.dz*
Tel : + 213 698533282

ISSN: 1112-2242 / EISSN: 2716-8247

inductance (INC) method (Emad et al. 2021; Shang et al. 2020; Owusu-Nyarko et al. 2021), and hill-climbing (Jately et al. 2021; Zhu et al. 2018). However, in the steady state, there are a lot of oscillations and power losses near the ideal position, which makes it difficult to respond quickly or accurately. Several advanced MPPT technologies have been developed in recent years to increase response time and accuracy, including neural networks (Ma et al. 2016; Messaltia et al. 2017; Robles Algarin et al. 2018), fuzzy logic controllers (Nabipour et al. 2017; Yilmaz et al. 2017; Chekired et al. 2017; Hai et al. 2022; Chen et al. 2016; Zaghba et al. 2015), neuro-fuzzy approaches (Zaghba et al. 2019; 2023), genetic algorithms (Borni et al. 2021), bee colony (Gong et al. 2023; Sathasivam et al. 2023; Atawi and Kassem, 2017), ant colony algorithms (Liu et al. 2023; Titri et al. 2017), particle swarm optimization (Zaghba et al. 2021; Koh et al. 2023; Refaat et al. 2023), and glow-worm swarm (Jin et al. 2017).

This work focuses in the first part on the optimization of the P&O-PI MPPT approach based on a soft computing technique called particle swarm optimization (PSO) to increase the follow-up time response of high-yield MPP. Furthermore, a study is conducted to analyze and contrast the efficiency of a photovoltaic conversion system linked to a two-axis solar tracker with that of a comparable fixed PV system. The obtained results proved that the importance and effectiveness of the photovoltaic system placed on a solar tracker were about 25%.

The manuscript is organized as follows: In Section 2, a grid-tied PV system description includes the designer of the proposed PSO-P&O-PI MPPT controller. Simulation results and discussion are presented in Section 3. The conclusion is presented in Section 4.

2. GRID-CONNECTED PV PLANT DESCRIPTION

The following schema shows the grid-connected solar system that will be studied in this research paper (see Fig 1). It is made up of the following blocks: PV field, boost converter, DC-Link, and two-level inverter connected to a three-phase grid.

The PV power field contains five strings. Each string contains 20 panels in series. Photovoltaic array electrical specifications are given in Table 1.

Table 1. Photovoltaic array electrical specifications

Power	6000 Wp
Voltage Vmpp	342 V
Current Impp	17.5 A
Short-circuit current (Isc)	19 A
Open-circuit voltage (Voc)	422 V
Number of Modules	100

2.1 DC-DC converter

A photovoltaic generator is attached to a boost converter. The boost converter state-space is given as (Zaghba et al. 2017a; 2017b; 2017c) :

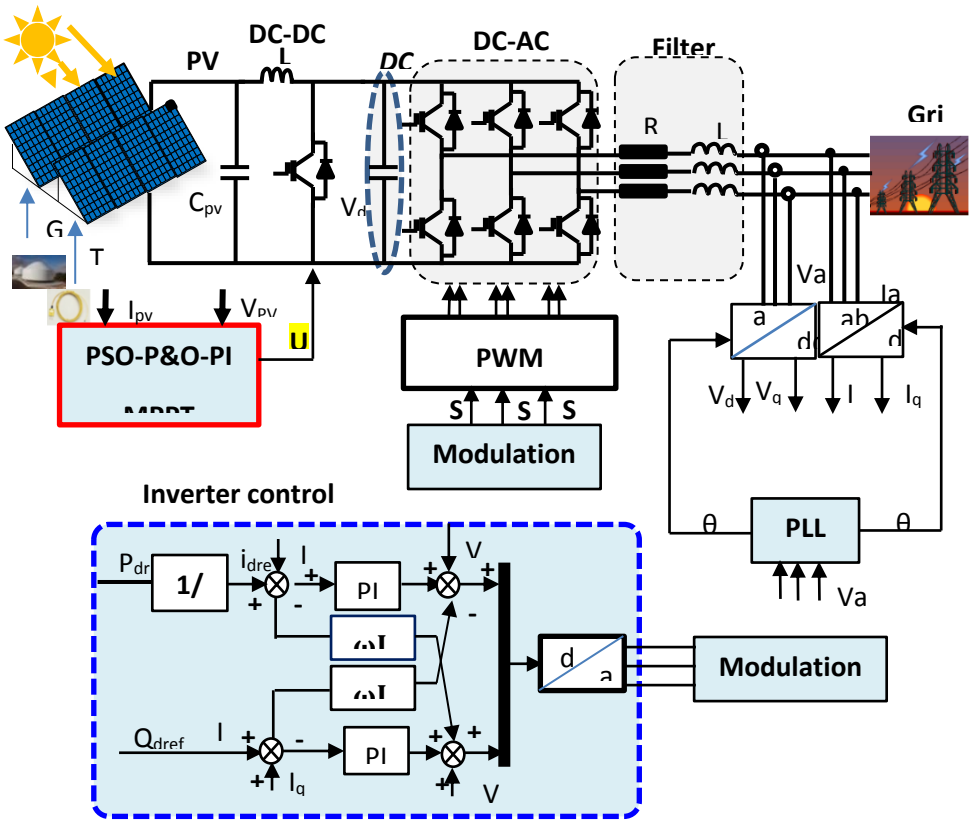

Fig 1. Two-stage grid-tied PV plant.

$$\begin{bmatrix} \dot{I}_L \\ \dot{V}_{dc} \end{bmatrix} = \begin{bmatrix} 0 & -\frac{1}{L}(1-D) \\ \frac{1}{C}(1-D) & -\frac{1}{C.R_L} \end{bmatrix} \begin{bmatrix} I_L \\ V_{dc} \end{bmatrix} + \begin{bmatrix} \frac{1}{L} \\ 0 \end{bmatrix} \quad (1)$$

$$\begin{cases} \dot{x_1} = -\frac{1-u}{L} x_2 + \frac{1}{L} D \\ \dot{x_2} = \frac{1-u}{C} x_1 + \frac{1}{RC} x_2 \end{cases} \quad (2)$$

Where u is the duty cycle, V_{pv} is the input voltage of the boost converter, I_L is the inductor current, C is the capacitance, R_L is the load resistance and V_{dc} is the DC link output.

2.2 Proposed MPPT technique

2.2.1 Perturbation and Observation (P&O) method

The perturbation and observation method (P&O) is the most widespread in the industrial environment because its algorithm is easy to implement. This process works by disturbing the system by increasing or decreasing the module's operating voltage and observing its effect on the output power of the array. Fig 2 shows the flowchart of the 'P&O' method algorithm.

Voltage (V) and current (I) measurements are used to calculate photovoltaic power. P (k) and P(k-1) are the recent PV and previous power of the photovoltaic module respectively. D (k) and D (k-1) are the recent PV and previous duty cycles respectively.

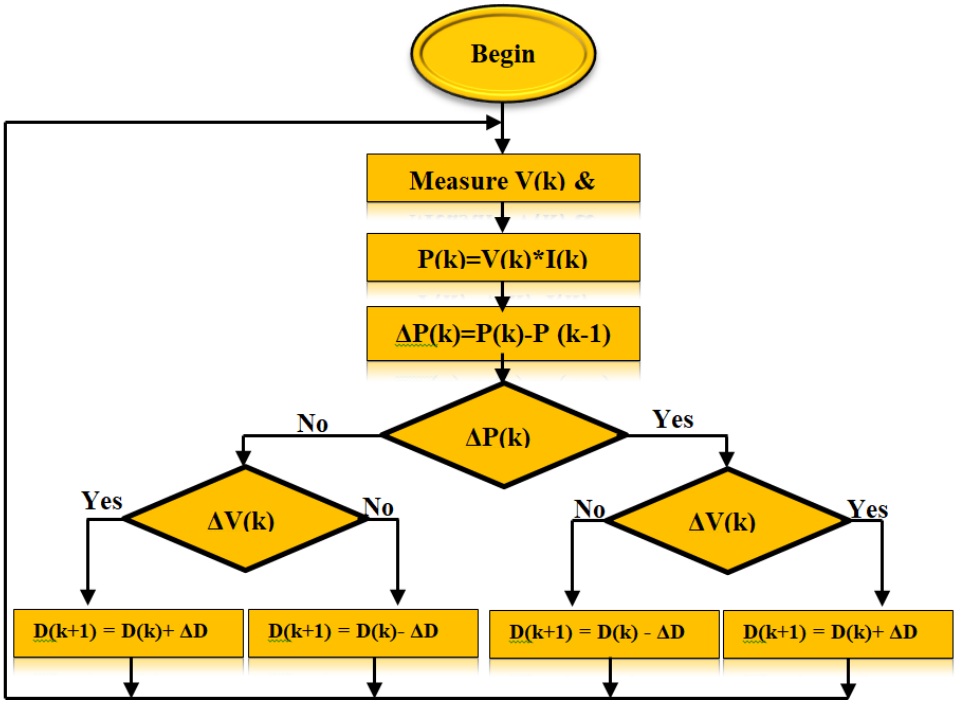

Fig 2. Flowchart of Perturb and observe algorithm.

2.2.2 Particle swarm optimization (PSO)

Most of the algorithms used to solve these optimization problems are population Metaheuristics. Among these, we are focused on optimization based on Particle Swarm Optimization (PSO), which appeared in 1995 [36]. PSO has attracted many researchers and has been exploited in different areas of optimization. This method is becoming more and more popular. It is inspired by the movements of animals that move in the form of a swarm (swarms of bees, flights of birds, fish). The benefits of this technique over classical or conventional techniques are the robustness and flexibility of its efficiency in a wide variety of problems. At time t, equation 3 determined the velocity vector.

$$v_{ij}(t) = wv_{ij}(t-1) + c_1 r_1 \left(p_{ijbest}(t-1) - x_{ij}(t-1)\right) + c_2 r_2((g_{ijbest}(t-1) - x_{ij}(t-1)) \quad (3)$$

$$j \in \{1, \dots, D\}$$

Equation 4 determines the position at time t of particle i:

$$x_{ij}(t) = x_{ij}(t-1) + v_{ij}(t), j \in \{1, \dots, D\} \quad (4)$$

Where:w is an inertia coefficient, c1 and c2 are acceleration coefficients, and r1 and r2 are two random numbers drawn uniformly in the range [0, 1]. The coefficient of inertia is given by

$$w = w_{max} - \left(\frac{w_{max} - w_{min}}{k_{max}}\right) \times k \quad (5)$$

Where: k_{max} and k are the number of iterations and the number of current iterations respectively. w_{min} and w_{max} are inertia coefficients.

2.2.3 Setting the PI controller using the PSO method for the MPPT command

Tuning the parameters of the PI controller can be considered an optimization problem when it comes to finding the optimal solution for the controller gains in a predefined search space to allow the system to follow the required reference. In this framework of analysis, we will apply the PSO technique to find the best combinations of the proportional and integral gains Kp_1, Kp_2, Ki_1, and Ki_2, proportional integrator regulators PI of voltage and current, which are used in the P & O MPPT command to extract the extreme power of a PV panel and improve its performance. The Laplace domain of the PI regulator is given by equation 6.

$$C(p) = K_p + \frac{K_i}{p} \tag{6}$$

Where: K_p: is a proportional gain, K_i: is the integral gain. We have an objective function (a cost function) to optimize in one direction or the other. The principle of the algorithm consists of moving these particles in the search space so that they find the best solution. The commonly used indices are defined as follows (Soufi et al. 2017):

Integration Absolute Error (IAE) is defined

$$IAE = \int_0^\infty |e(t)|dt \tag{7}$$

Integral Time Absolute Error (ITAE) is given by:

$$ITAE = \int_0^\infty t|e(t)|dt \tag{8}$$

Integrated Squared Error (ISE) is defined by:

$$ISE = \int_0^\infty e^2 dt \tag{9}$$

Where e(t) is the error value. The objective of the PSO algorithm is to reduce the determined objective function (F), according to the following criteria:

$$e_1(i) = \int \left(V_{pv\_ref} - V_{pv}\right)^2 dt \tag{10}$$

$$e_2(i) = \int \left(I_{pv\_ref} - I_{pv}\right)^2 dt \tag{11}$$

$$F = \sum_{i}^{N} |e_1(i)| + |e_2(i)| \tag{12}$$

Where: V_{pv_ref} and I_{pv_ref} are the reference voltage and current respectively,V_{pv} and I_{pv} the voltage and current delivered by the module under STC conditions. The PSO algorithm is employed to determine the four gains of the PI regulator (Kp_1, Kp_2, Ki_1, and Ki_2), based on the two errors (the first error is between the reference voltage and the maximum voltage delivered by the module and the second error is between the reference current and the maximum current produced by the module) where the particles are decoded in four dimensions for Kp1, Kp2, Ki1, and Ki2. Fig 3 depicts the global block diagram of the PSO approach for adjusting the gains (Kp_1, Kp_2, Ki_1, and Ki_2) of the two PI regulators.

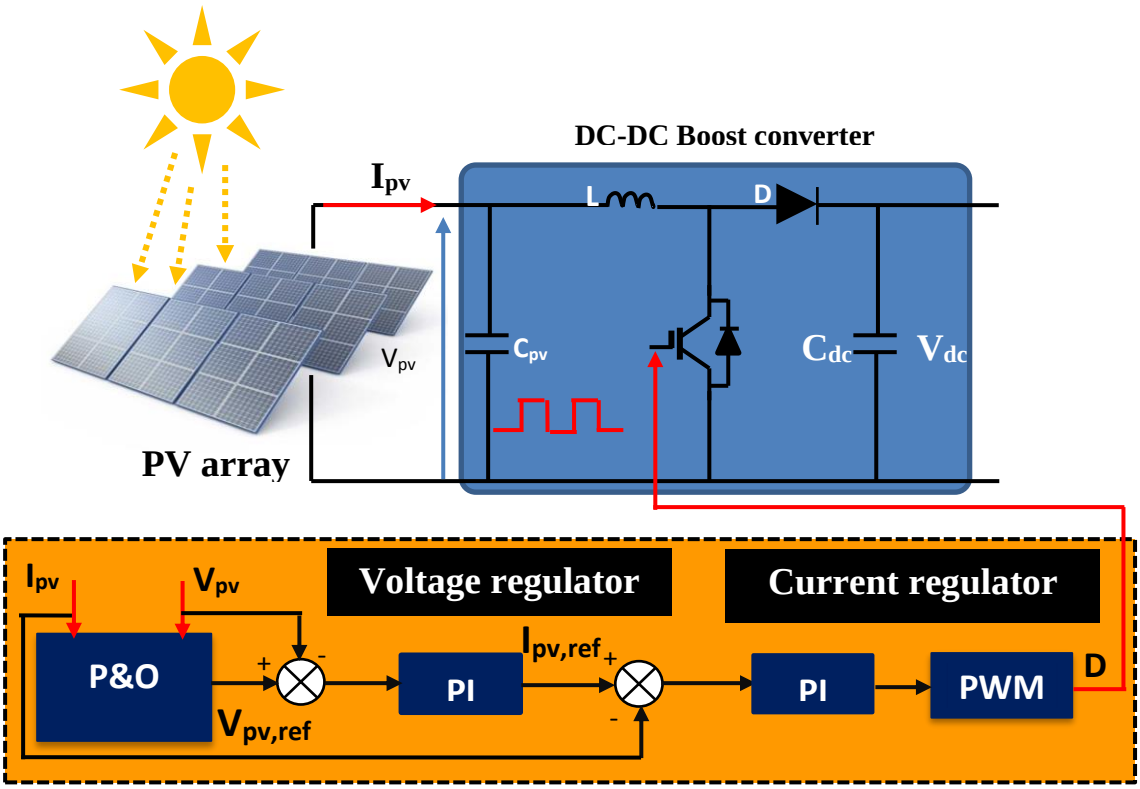

Fig 3. Diagram of PV plant with proposed MPPT control

2.3 Grid side

The voltage of a balanced three-phase power network is given by the following equations (Menadi et al. 2015; Boudaraia et al. 2016):

$$\begin{cases} e_a = E_m \cos wt \\ e_b = E_m \cos(wt - \frac{2\pi}{3}) \\ e_c = E_m \cos(wt + \frac{2\pi}{3}) \end{cases} \quad (13)$$

E_m : The maximum voltage value. The grid voltage at the grid side of the converter is given by (13)

$$\begin{cases} e_a = L\frac{d}{dt}i_a + Ri_x + v_a \\ e_b = L\frac{d}{dt}i_b + Ri_y + v_b \\ e_c = L\frac{d}{dt}i_c + Ri_z + v_c \end{cases} \quad (14)$$

Using a coordinate transformation, the equation becomes as follows.

$$\begin{pmatrix} \frac{di_d}{dt} \\ \frac{di_q}{dt} \end{pmatrix} = \frac{1}{L}\begin{pmatrix} -R & wL \\ wL & -R \end{pmatrix}\begin{pmatrix} i_d \\ i_q \end{pmatrix} - \frac{1}{L}\begin{pmatrix} e_d \\ e_q \end{pmatrix} + \frac{1}{L}\begin{pmatrix} v_d \\ v_q \end{pmatrix} \quad (15)$$

The control voltage equations are as follows

$$\begin{cases} v_d = (K_p + \frac{K_i}{S})(i_{dref} - I_d) - wLi_q + e_d \\ v_q = (K_p + \frac{K_i}{S})(i_{qref} - I_q) + wLi_d + e_q \end{cases} \quad (16)$$

3. SIMULATION RESULTS

The power plant with a capacity of 6 kWp under the nominal conditions of STC is simulated below (both with and without solar tracking). It comprises two cascade conversion stages. The first stage is "continuous" and has five parallel module branches. Each branch has 20 MSX 60 series modules connected in serial as well as a boost converter that elevates the generator's ideal voltage to a level appropriate for the continuous bus. The second stage option comprises an inverter connected to the grid.

3.1 Abrupt Variation of Irradiation

The output of a PV array during an abrupt change in irradiation, G=500 W/m2, from t=0 to 0.3 seconds is shown in Fig 4. From t=0.3s to t=0.6s, G is 300 W/m2, and from t=0.6s to 1s, it is 1000 W/m².

3.2 Real solar irradiation profile

The proposed control device consists mainly of two control blocks (current and voltage blocks). The parameters of the system to be simulated are summarized in Table 2. The indicators of the PSO technique are displayed in Table 3. The variations of the objective function and the variations of the optimal gains Kp1, Ki1, Kp2, and Ki2 during the simulation are depicted respectively in Fig. 5 and Fig. 6.

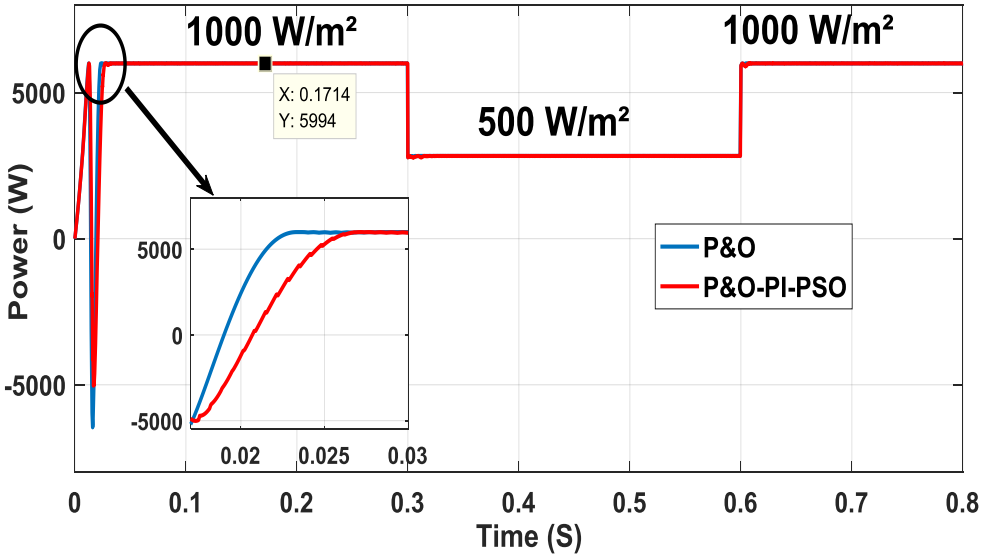

Fig 4. PV array power

Table 2. Specifications for grid-connected power plants

Boost converter	DC bus	Inverter	PI	Filter	Grid
C= 1000 μF L= 50 mH fs=4500 Hz	Vdc=800 V Cdc= 2.2 mF	fs=15 kHz	Kp=9 Ki=300	Lf= 3 mH Rf=0.1Ω	Vr=380 V f=50 Hz

Table 3. Indicators of the PSO technique

The size of the swarm	15
The maximum number of iterations	20
c_1=c_2	2
w_{max}	0.9
w_{min}	0.4

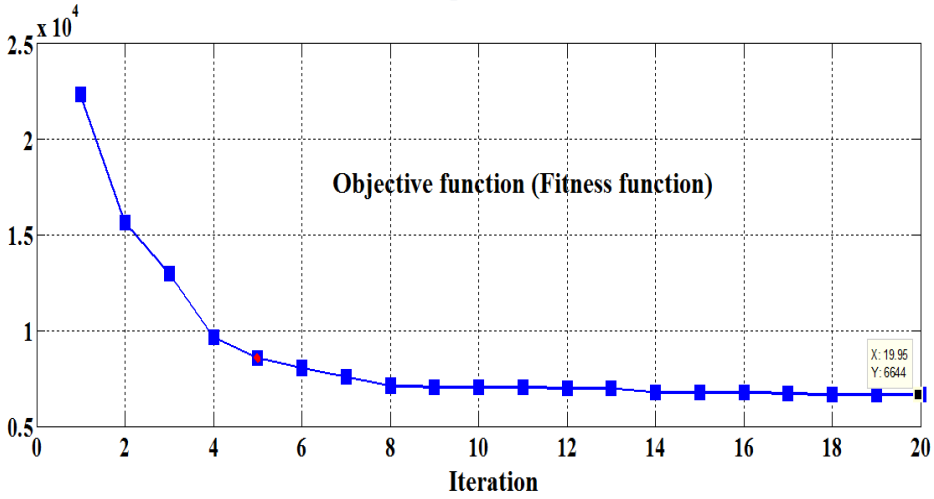

Fig 5. Variations of the objective function.

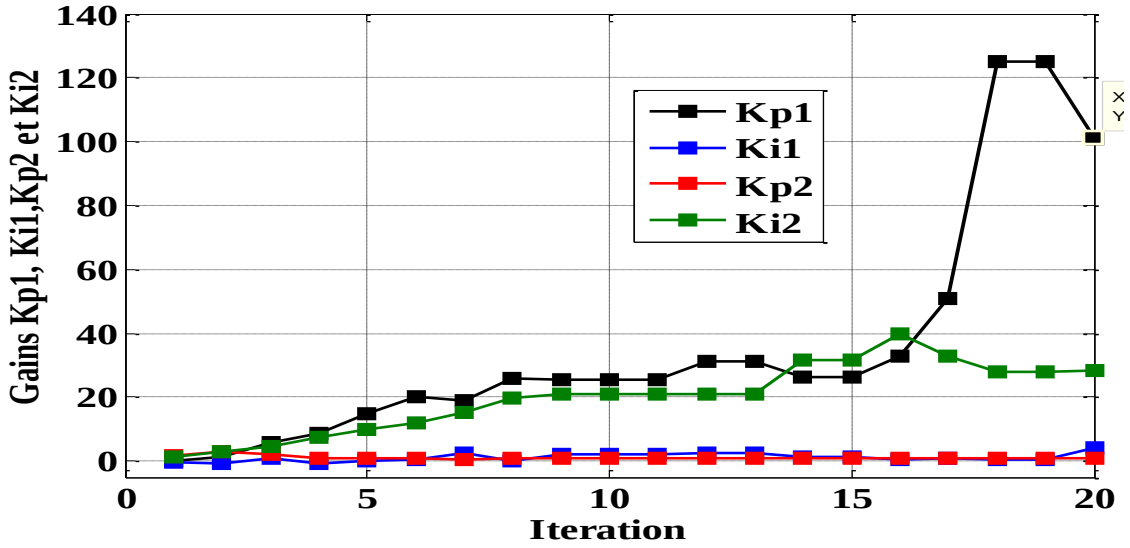

Fig 6. Variations of the optimal gains Kp_1, Ki_1, Kp_2, and Ki_2.

The optimal value of the objective function is 6.6436e + 03 and the optimal gains are Kp1 = 100.90, Ki1 = 4.34, Kp2 = 0.77, and Ki2 = 28.22, which are clearly shown in Fig .6. The optimal indicators of the P&O-PI controller employed by PSO are summarized in Table 4.

Table 4. Tuning factors of the P&O-PI controller employed by PSO.

Factors	Kp_1	Ki_1	Kp_2	Ki_2
P&O-PI	100.90	4.34	0.77	28.22

To study the behavior of our system under the real climatic changes of irradiation in the Matlab Simulink environment, we have chosen two typical days. The weather station established at the applied research unit in renewable energies (URAER/CDER) provided the actual meteorological data for global irradiations on the fixed tilt (32°) used. The global solar irradiation with a two-axis tracker based on the Liu & Jordan model. These data were taken from an online Web application designed by the Development of Renewable Energies Center [http://data.cder.dz:81].

Figure 7 highlights the daily variations of the daily solar radiation for the two systems under study (solar and stationary tracking). The daily solar radiation captured by a sun tracker is drawn in red, while that of the fixed PV plant is blue. An examination shows that for a clear sky, daytime solar radiation changes in Gaussian form between 0 W/m^2 and 1000 W/m^2. The values are weak at sunrise and sunset and peak at midday (noon). We find that in the case of biaxial solar tracking, the solar radiation is much higher than in the inclined plane.

Figures 8 and 9 depict the evolution of the current and the daily power of the PV array for the two PV systems (with and without a sun tracker). An examination of the two figures shows that, for a clear sky, the current and power change during the day in the form of a Gaussian. The values are weak at sunrise and sunset and peak at midday (noon). The current profile increases gradually from zero until reaching the maximum value of 20A which corresponds to the extreme value of radiation of 1000 W/m^2 seen at midday (see Fig 8). The power profile gradually increases from zero until reaching the maximum value of 6 kWp which corresponds to the extreme value of radiation of 1000 W/m^2 seen at midday (see

Fig.9). Fig. 10 shows a comparative diagram of PV electricity production output (gained energy) from a PV plant with a sun tracker to a similar fixed installation (32°). The purpose is to visualize electrical characteristics at the output of the PV field and the benefits of employing a PV plant with a sun tracker. According to the outcomes, it appears that all the electrical quantities (powers, voltages, and currents) to optimize the photovoltaic generator converge well with their references after a reasonable response time (0.01s) relative to the dynamics of the variation of the irradiation profile.

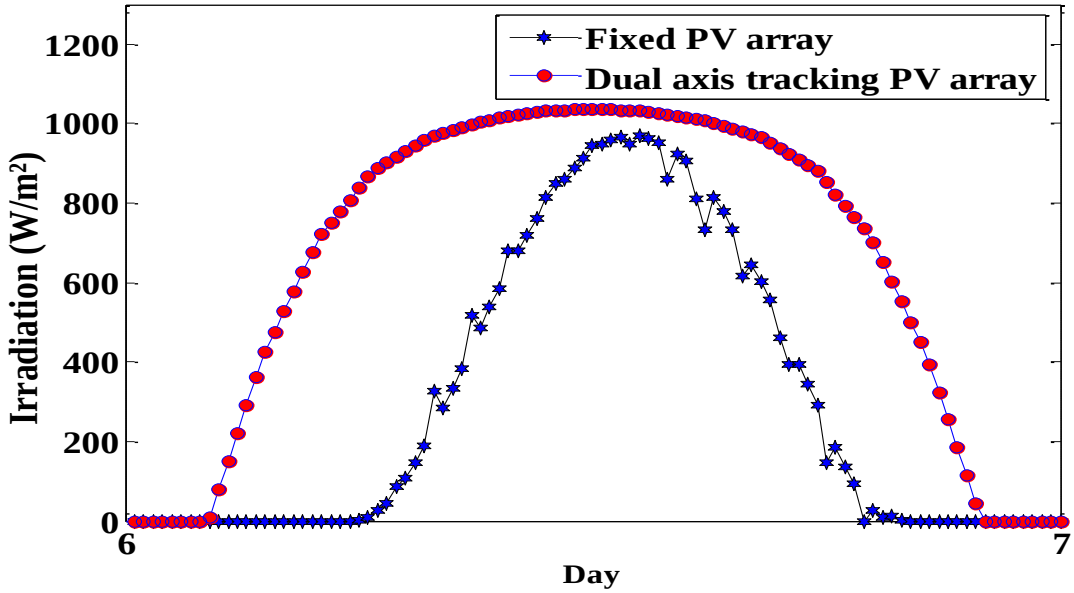

(a)

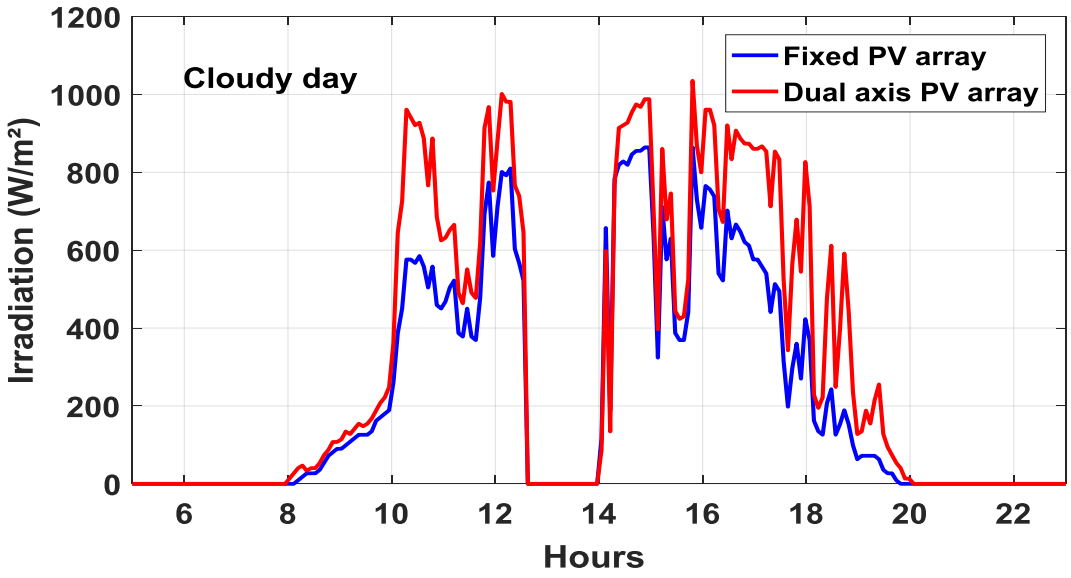

(b)

Fig 7. Irradiation profile on a fixed plane and 2-axis solar tracker (a) clear sky day (b) cloudy day

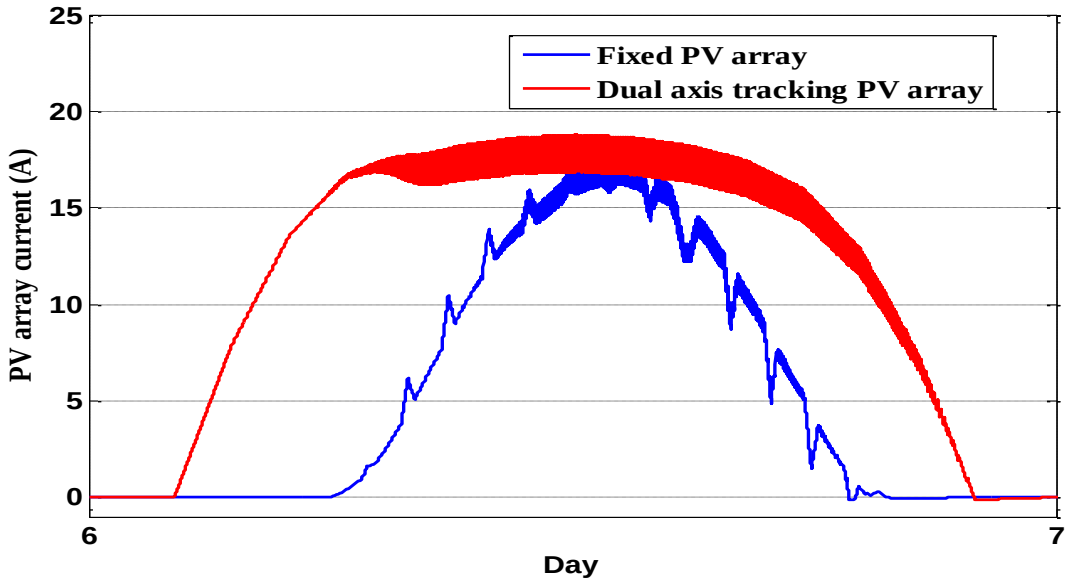

(a)

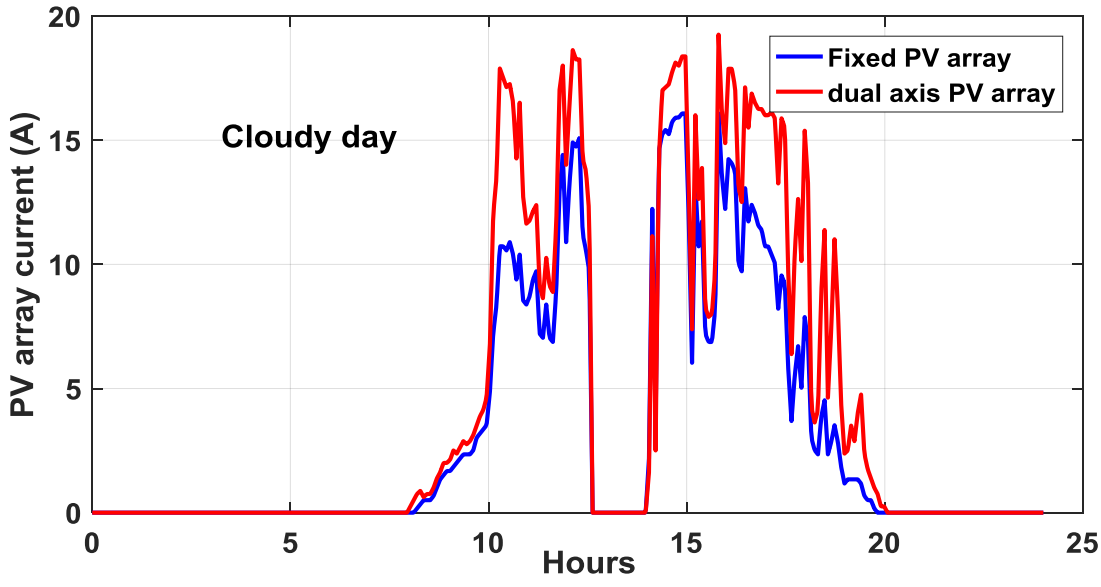

(b)

Fig 8. Characteristics of PV generator currents. (a) clear sky day (b) cloudy day

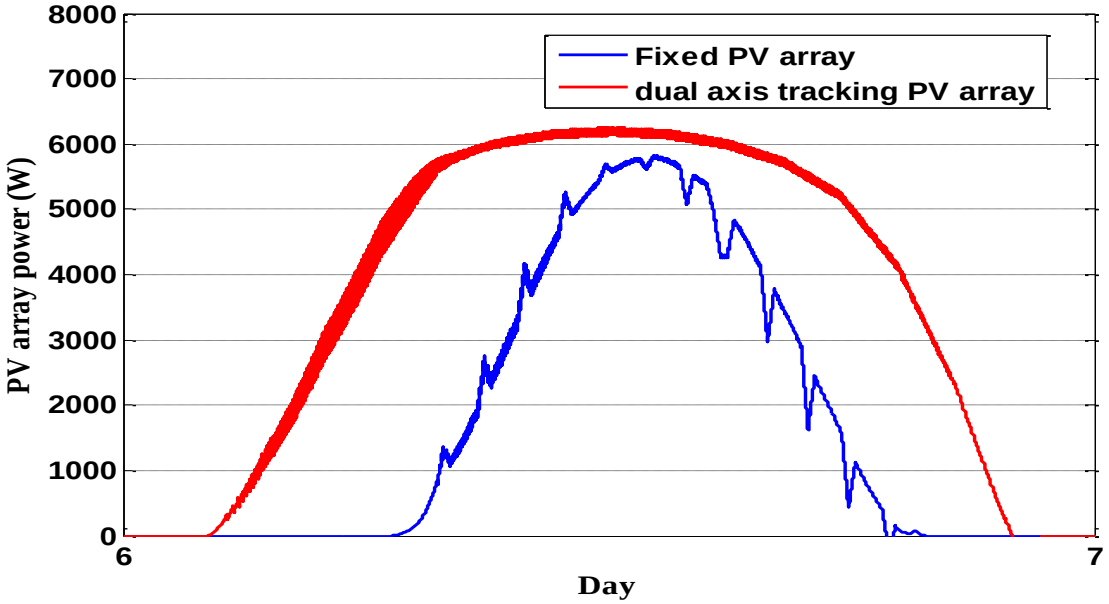

(a)

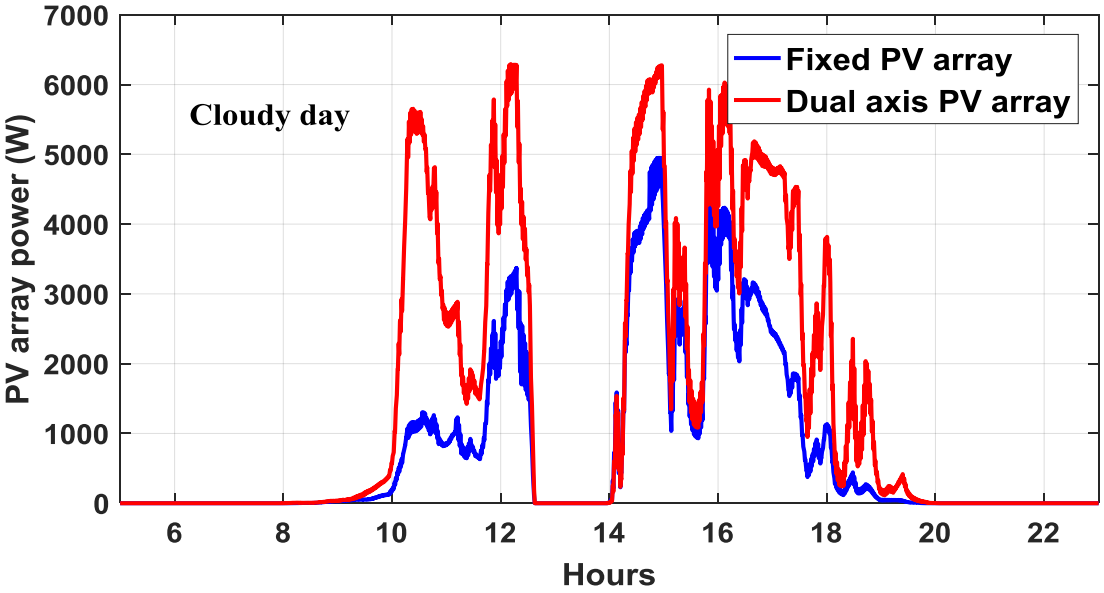

(b)

Fig 9. Characteristics of PV generator powers (a) clear sky (b) cloudy day.

The bus voltage is maintained at the reference voltage for both grid-tied photovoltaic systems (with and without a sun tracker) regardless of variations in light (800 V), as illustrated in Fig.11.

The characteristics of the three-phase currents (Iabc) and the current (Id) injected into the grid are shown in Fig. 12. According to the simulation results shown below, the network's current injection converges well with its references (20 A) after a quicker response time (0.01 s), which is consistent with the dynamics of the illumination profile.

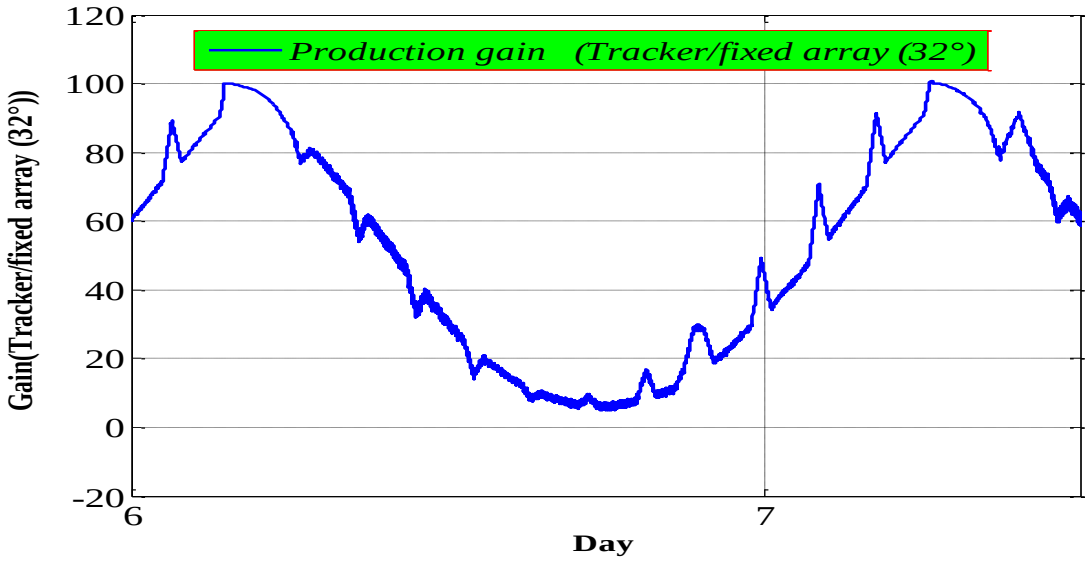

Fig 10. The gain of production (Sun tracker vs fixed inclined PV system).

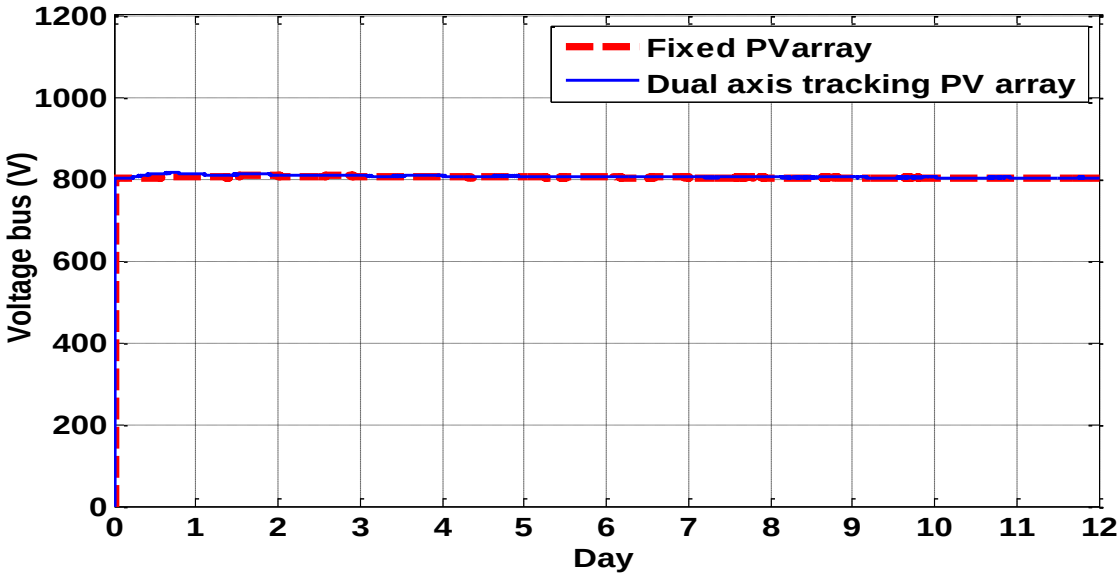

Fig 11. DC link voltage.

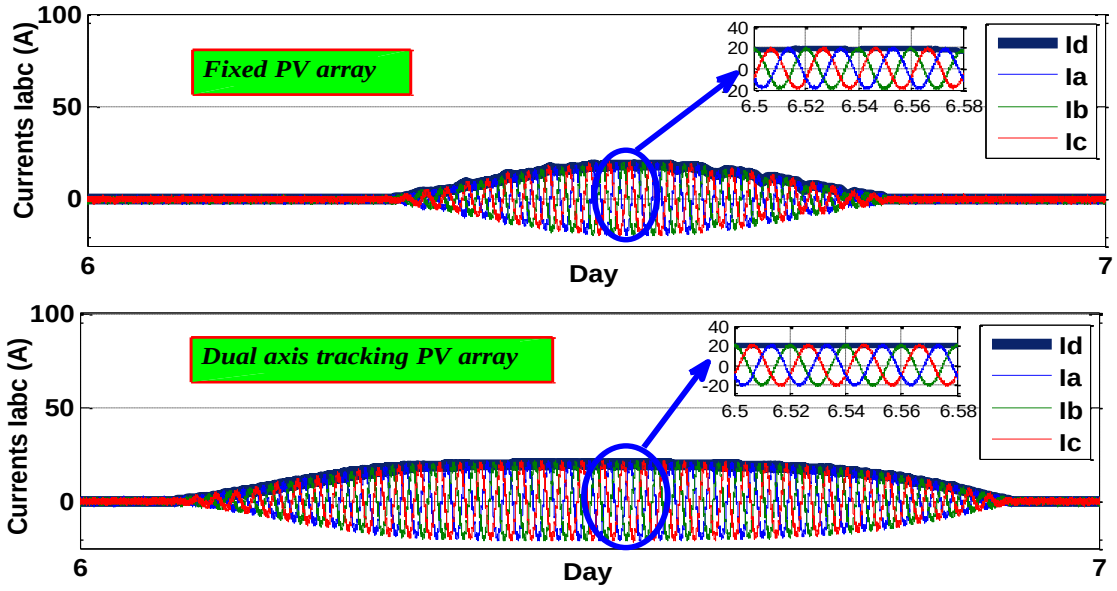

Fig 12. Currents injected into the network and their zoom waveforms.

Fig 13 shows the measured currents (Id_mes and Iq_mes) and the reference currents (Id_ref and Iq_ref).

A balanced three-phase system is created by the network's three-phase voltages (Fig. 14), which have a sinusoidal shape, have the same frequency of 50 Hz, are phase-shifted by 2/3, and have the same RMS value of 220V.

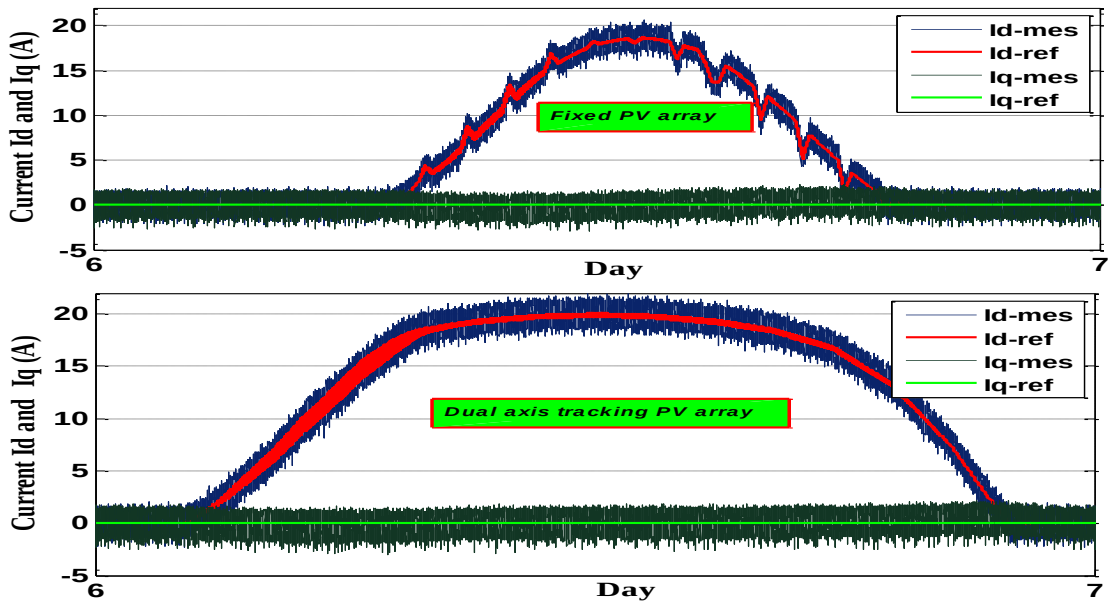

Fig 13. Measured currents and their references.

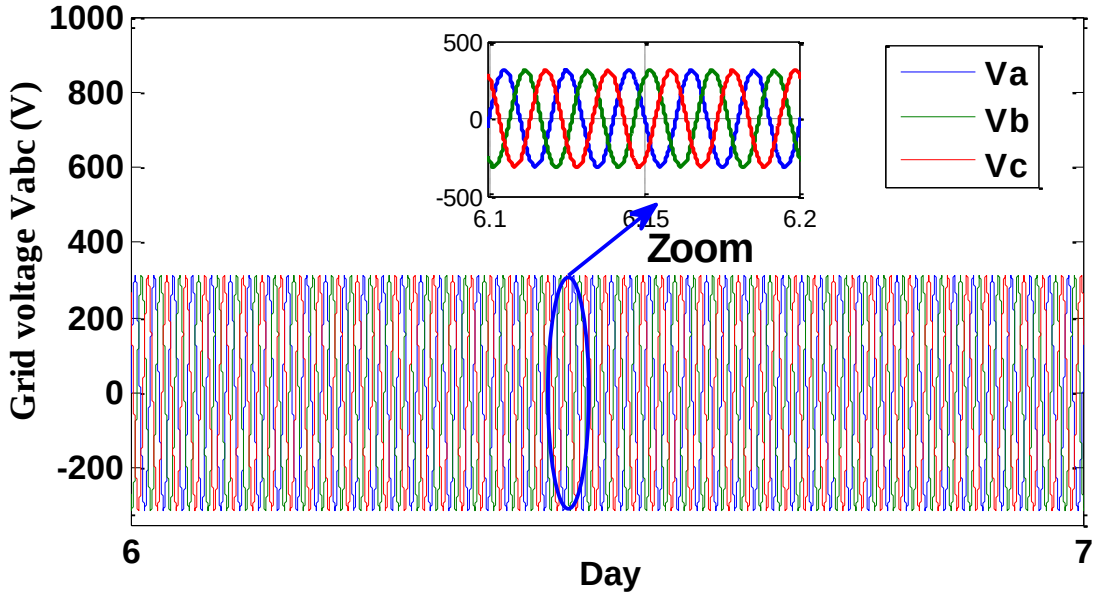

Fig 14. Characteristics of three-phase main voltages.

Figure 15 depicts the characteristics of the network's total active power injection as well as its zero reactive power. A better decoupling between active and reactive power is also depicted in the picture. Throughout all irradiation fluctuations, the active power stays within the boundaries of its reference values. We can infer from the simulation results used in this study that the PV plant controlled by the P&O-PI approach optimized with PSO adapts to changes in the irradiation profile and demonstrates its effectiveness not only for tracking the maximum power point but also for response time and low fluctuation.

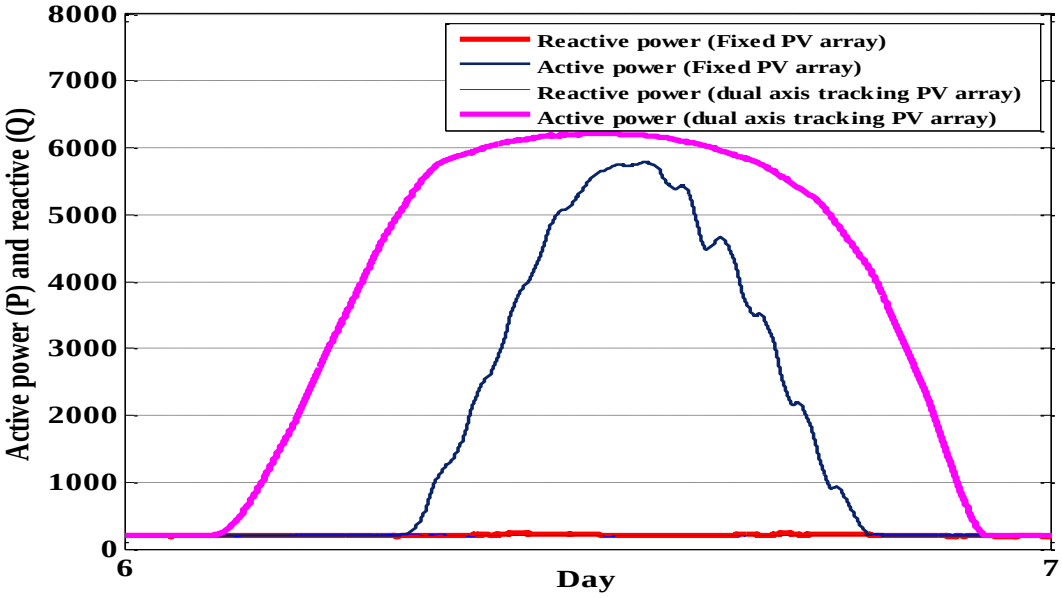

Fig 15. Active and reactive powers injected into the grid.

The PSO-P&O-PI MPPT algorithm delivers a significant improvement in tracking efficiency of 99.90%, a time response of 0.023 s, and reduced oscillation when compared to the earlier techniques. Table 5 demonstrates how peer benchmarking of MPPT algorithms verifies the specified technique.

Table 5.Performances comparison between PSO-P&O-PI MPPT and other methods

Methods	MPP of P-V curve (W)	Extracted PV power (W)	Power loss		Efficiency (%)	Convergence time (Sec)	Reference
			(W)	(%)			
PSO-P&O-PI	6000	5994	6	0.10	99.90	0.023	Present study
CSA	325.5	325.4	0.1	0.03	99.97	0.31	Houam et al. (2021)
PSO	1260	1244	16	1.27	98.7	0.47	Hafeez et al. (2022)
InC	864	863.1	0.9	0.10	99.90	0.52	Sarwar et al. (2022)
Firefly algorithm (FA)	864	852	12	1.39	98.61	0.60	Sarwar et al. (2022)
Ant Colony Optimization (ACO)	864	862.2	1.8	0.21	99.76	0.53	Sarwar et al. (2022)
Dragon fly Optimization (DFO)	864	863.3	0.7	0.08	99.77	0.53	Sarwar et al. (2022)

4. CONCLUSION

In this paper, we recommend the P&O-PI technique that has been optimized with PSO approaches. To determine the current and voltage regulators' ideal gain, which correlates to a PV system's maximum power point, the particle swarm optimization (PSO) method is used. The simulation results demonstrate the best performance and the MPPT controller is capable of promptly maintaining the PV system's maximum working point and its amount of energy, increasing efficiency. Two distinct PV system types—fixed and equipped with sun trackers—that are connected to the grid are compared. Enhancing the electrical energy gain (acquired energy) of the solar panel concerning a stationary PV system is the goal. We have shown the value of using the sun tracker when generating power, especially during the midday hours of the day, with an estimated 25% energy gain.

REFERENCES

Alik R and Jusoh A. (2017). Modified perturb and observe (P&O) with checking algorithm under various solar irradiation. Solar Energy 148: 128–39. DOI: 10.1016/j.solener.2017.03.064.

Atawi I E and Kassem A M. (2017). Optimal control based on maximum power point tracking (MPPT) of an autonomous hybrid photovoltaic/storage system in microgrid applications. Energies 10(15): 1–14. https://doi.org/10.3390/en10050643.

Borni, A., Bechouat, M., Bessous, N., Bouchakour, A., Laid, Z. & Zaghba, L. (2021). Comparative Study of P&O and Fuzzy MPPT Controllers and Their Optimization Using PSO and GA to Improve Wind Energy System. *International Journal for Engineering Modelling, 34* (2 Regular Issue), 55-76. https://doi.org/10.31534/engmod.2021.2.ri.05d.

Boudaraia K, Mahmoudi H, El Azzaoui M. (2016). Modeling and Control of Three Phases Grid Connected Photovoltaic System, Renewable and Sustainable Energy Conference (IRSEC), International, DOI: 10.1109/IRSEC.2016.7984004.

Chekired Fathia, Achour Mahrane, Zoubeyr Samara, Madjid Chikh, Abderrazak Guenounou, Aissa Meflah, (2017) Fuzzy logic energy management for a photovoltaic solar home, Energy Procedia, Volume 134, 2017, Pages 723-730, ISSN 1876-6102, https://doi.org/10.1016/j.egypro.2017.09.566.

Chen YT, Jhang YC, and Liang RH. (2016). A fuzzy-logic based auto-scaling variable stepsize MPPT method for PV systems. Solar Energy, Vol. 126, pp.53–63. https://doi.org/10.1016/j.solener.2016.01.007.

Danandeh M A and Mousavi S M. (2018). Comparative and comprehensive review of maximum power point tracking methods for PV cells. Renewable and Sustainable Energy Reviews Elsevier, vol. 82 (P3), pages 2743-2767. https://doi.org/10.1016/j.rser.2017.10.009.

Emad M. Ahmed, Hojat Norouzi, Salem Alkhalaf, Ziad M. Ali, Sajjad Dadfar, Noritoshi Furukawa, (2021). Enhancement of MPPT controller in PV-BES system using incremental conductance along with hybrid crow-pattern search approach based ANFIS under different environmental conditions, Sustainable Energy Technologies and Assessments, Volume 50,2022,101812, ISSN 2213-1388, https://doi.org/10.1016/j.seta.2021.101812.

Gong, L., Guolian Hou, Congzhi Huang, (2023). A two-stage MPPT controller for PV system based on the improved artificial bee colony and simultaneous heat transfer search algorithm, ISA Transactions, Volume 132,2023, Pages 428-443, ISSN 0019-0578,https://doi.org/10.1016/j.isatra.2022.06.005.

Hafeez, Muhammad Annas, Ahmer Naeem, Muhammad Akram, Muhammad Yaqoob Javed, Aamer Bilal Asghar, and Yong Wang. (2022). A Novel Hybrid MPPT Technique Based on Harris Hawk Optimization (HHO) and Perturb and Observer (P&O) under Partial and Complex Partial Shading Conditions, Energies 15, no. 15: 5550. https://doi.org/10.3390/en15155550.

Hassan, A., Octavian Bass, Mohammad A.S. Masoum, (2023). An improved genetic algorithm based fractional open circuit voltage MPPT for solar PV systems, Energy Reports, Volume 9,2023, Pages 1535-1548, ISSN 2352-4847,https://doi.org/10.1016/j.egyr.2022.12.088.

Houam, Y., Terki, A. & Bouarroudj, N. (2021). An Efficient Metaheuristic Technique to Control the Maximum Power Point of a Partially Shaded Photovoltaic System Using Crow Search Algorithm (CSA). J. Electr. Eng. Technol. 16, 381–402. (2021). https://doi.org/10.1007/s42835-020-00590-8.

Huang Y P and Hsu S Y. (2016). A performance evaluation model of a high concentration photovoltaic module with a fractional open circuit voltage-based maximum power point tracking algorithm. Computers & Electrical Engineering 51: 331–42. https://doi.org/10.1016/j.compeleceng.2016.01.009.

Jin Y, Hou W, Li G and Chen X. (2017). A Glowworm Swarm optimization-based maximum power point tracking for photovoltaic/thermal systems under non-uniform solar irradiation and temperature distribution. Energies 10(4): 1–13. https://doi.org/10.3390/en10040541.

Koh, J. S., Tan, R. H. G., Lim, W. H. and Tan, N. M. L. (2023). A Modified Particle Swarm Optimization for Efficient Maximum Power Point Tracking Under Partial Shading Condition," in IEEE Transactions on Sustainable Energy, vol. 14, no. 3, pp. 1822-1834, July 2023, doi: 10.1109/TSTE.2023.3250710.

Kota VR and Bhukya MN. (2017)..A novel linear tangents based P&O scheme for MPPT of a PV system. Renewable and Sustainable Energy Reviews 71: 257–67. DOI: 10.1016/j.rser.2016.12.054.

Liu Chao, Lei Wu, Wensheng Xiao, Guangxin Li, Dengpan Xu, Jingjing Guo, Wentao Li, (2023). An improved heuristic mechanism ant colony optimization algorithm for solving path planning, Knowledge-Based Systems, Volume 271,2023,110540, ISSN 0950-7051,https://doi.org/10.1016/j.knosys.2023.110540.

Ma S, Chen M, Wu J, Huo W, and Huang L. (2016). Augmented nonlinear controller for maximum power-point tracking with artificial neural network in grid-connected photovoltaic systems. Energies 9(12): 1–24. https://doi.org/10.3390/en9121005.

Menadi A, et al. (2015). Implementation of fuzzy-sliding mode based control of a grid connected photovoltaic system. ISA Transactions, http://dx.doi.org/10.1016/j.isatra.2015.06.009.

Messaltia S, Harrag A and Loukriz A. (2017). A new variable step size neural networks MPPT controller: review, simulation and hardware implementation. Renewable and Sustainable Energy Reviews 68(1): 221–33. https://doi.org/10.1016/j.rser.2016.09.131.

Nabipour M, Razaz M, Seifossadat S G and Mortazavi S S. (2017). A new MPPT scheme based on a novel fuzzy approach. Renewable and Sustainable Energy Reviews 74: 1147–69. DOI:10.1016/J.RSER.2017.02.054.

Owusu-Nyarko, I., Elgenedy, M.A.; Abdelsalam, I.; Ahmed, K.H. (2021). Modified Variable Step-Size Incremental Conductance MPPT Technique for Photovoltaic Systems. *Electronics* 2021, *10*, 2331. https://doi.org/10.3390/electronics10192331.

Refaat, A., Abd-Elwahab Khalifa, Mohamed Mohamed Elsakka, Yasser Elhenawy, Ahmed Kalas, Medhat Hegazy Elfar, (2023). A novel metaheuristic MPPT technique based on enhanced autonomous group Particle Swarm Optimization Algorithm to track the GMPP under partial shading conditions - Experimental validation, Energy Conversion and Management, Vol. 287, 2023, 117124, https://doi.org/10.1016/j.enconman.2023.117124.

Robles Algarín C, Sevilla Hernández D and Restrepo Leal D. (2018). A low-cost maximum power point tracking system based on neural network inverse model controller. electronics 7(1): 1–17. DOI: 10.3390/electronics7010004.

Sarwar, Sajid, Muhammad Yaqoob Javed, Mujtaba Hussain Jaffery, Jehangir Arshad, Ateeq Ur Rehman, Muhammad Shafiq, and Jin-Ghoo Choi. (2022). A Novel Hybrid MPPT Technique to Maximize Power Harvesting from PV System under Partial and Complex Partial Shading, Applied Sciences 12, no. 2: 587. https://doi.org/10.3390/app12020587.

Sathasivam Karthikeyan, Ilhan Garip, Saeed Hassan Saeed, Yaser Yais, Ali Ihsan Alanssari, Ali Adhab Hussein, Jenan Ali Hammoode & Alaa M. Lafta (2023). A Novel MPPT Method Based on PSO and ABC Algorithms for Solar Cell, Electric Power Components and Systems, DOI: 10.1080/15325008.2023.2228795.

Shang, L., Guo, H. & Zhu, W. (2020). An improved MPPT control strategy based on incremental conductance algorithm. (2020). *Prot Control Mod Power Syst* **5**, 14 (2020). https://doi.org/10.1186/s41601-020-00161-z.

Soufi Youcef, Mohcene Bechouat, Sami Kahla, (2017). Fuzzy-PSO controller design for maximum power point tracking in a photovoltaic system, International Journal of Hydrogen Energy, Volume 42, Issue 13, 2017, Pages 8680-8688, ISSN 0360-3199, https://doi.org/10.1016/j.ijhydene.2016.07.212.

Tao Hai, Jincheng Zhou, Kengo Muranaka, (2022). An efficient fuzzy-logic based MPPT controller for grid-connected PV systems by farmland fertility optimization algorithm, Optik, Volume 267, 2022, 169636, ISSN 0030-4026,https://doi.org/10.1016/j.ijleo.2022.169636.

Titri S, Larbes C, Toumi K Y and Benatchba K. (2017). A new MPPT controller based on the Ant colony optimization algorithm for photovoltaic systems under partial shading conditions. Applied Soft Computing 58: 465–79. https://doi.org/10.1016/j.asoc.2017.05.017.

Vibhu Jately, Brian Azzopardi, Jyoti Joshi, Balaji Venkateswaran V, Abhinav Sharma, Sudha Arora, (2021). Experimental Analysis of hill-climbing MPPT algorithms under low irradiance levels, Renewable and Sustainable Energy Reviews, Volume 150,2021,111467, ISSN 1364-0321, https://doi.org/10.1016/j.rser.2021.111467.

Vijayakumari, A. (2021). A non-iterative MPPT of PV array with online measured short circuit and open circuit quantities, Journal of King Saud University - Engineering Sciences, Volume 33, Issue 3,2021, Pages 176-185, ISSN 1018-3639,https://doi.org/10.1016/j.jksues.2020.04.007.

Yilmaz U, Kircay A and Borekci S. (2018). PV system fuzzy logic MPPT method and PI control as a charge controller. Renewable and Sustainable Energy Reviews 81(1): 994–1001. DOI:10.1016/J.RSER.2017.08.048.

Zaghba L. et al., (2015). Robust tracking with fuzzy sliding mode control strategy for grid connected photovoltaic system, (2015). 3rd International Renewable and Sustainable Energy Conference (IRSEC), 2015, pp. 1-6, doi: 10.1109/IRSEC.2015.7455022.

Zaghba L , Borni A , Khennane M , Terki N, Fezzani A , Bouchakour A, Hadj Mahamed I, Oudjana S H. (2017a). Experimental typical meteorological years to study energy performance of a PV grid-connected system, Energy procedia, 119, 297-307. https://doi.org/10.1016/j.egypro.2017.07.085.

Zaghba L, Khennane M, Borni A, Fezzani A. (2017b). Control and performance analysis of grid connected photovoltaic systems of two different technologies in a desert environment, Leonardo Electronic Journal of Practices and Technologies, ISSN 1583-1078, Issue 31, July-December 2017 p. 111-128.

Zaghba L, Khennane M, Terki N, Borni A, Bouchakour A, Fezzani A, Hadj Mahamed I, and Oudjana S.H. (2017c). The effect of seasonal variation on the performances of grid-connected photovoltaic system in southern Algeria, AIP Conference Proceedings 1814, 020005; https://doi.org/10.1063/1.4976224.

Zaghba L. et al., (2019). An enhancement of grid connected PV system performance based on ANFIS MPPT control and dual axis solar tracking. (2019). 1st International Conference on Sustainable Renewable Energy Systems and Applications (ICSRESA), 2019, pp. 1-6, doi: 10.1109/ICSRESA49121.2019.9182591.

Zaghba, L., Khennane, M., Borni, A., & Fezzani, A. (2021). Intelligent PSO-Fuzzy MPPT approach for Stand-Alone PV System under Real Outdoor Weather Conditions. Algerian Journal of Renewable Energy and Sustainable Development, 3(01), 1-12. Retrieved from https://ajresd.univ-adrar.edu.dz/index.php?journal=AJRESD&page=article&op=view&path[]=100.

Zaghba, L., Abdelhalim Borni, Messaouda Khennane & Amor Fezzani (2023). Modeling and simulation of novel dynamic control strategy for grid-connected photovoltaic systems under real outdoor weather conditions using Fuzzy–PI MPPT controller, International Journal of Modelling and Simulation, 43:5, 549-558, DOI:10.1080/02286203.2022.2094663.

Zhu, Weiwei, Li-qun Shang, Pengwei Li and Hangchen Guo. (2018). Modified hill climbing MPPT algorithm with reduced steady-state oscillation and improved tracking efficiency. *The Journal of Engineering* (2018). DOI:10.1049/JOE.2018.8337.